



Monolithic integration of light-emitting diodes and power metal-oxide-semiconductor channel high-electron-mobility transistors for light-emitting power integrated circuits in GaN on sapphire substrate

Z. Li,^{1,a)} J. Waldron,^{1,b)} T. Detchprohm,^{2,c)} C. Wetzel,² R. F. Karlicek, Jr.,¹ and T. P. Chow¹

¹Department of Electrical, Computer, and Systems Engineering, Rensselaer Polytechnic Institute, Troy, New York 12180, USA

²Department of Physics, Applied Physics, and Astronomy, Rensselaer Polytechnic Institute, Troy, New York 12180, USA

(Received 30 March 2013; accepted 1 May 2013; published online 16 May 2013)

We report the demonstration of monolithically integrated light-emitting diodes (LEDs) and power metal-oxide-semiconductor channel high-electron-mobility transistors (HEMTs) in GaN. The structure comprised a direct epitaxial integration of layers typical for a GaN-based LED grown directly on top of the layers of a GaN-based HEMT. The layers were then fabricated into a serially connected pair of GaN LED and metal-oxide-semiconductor-gated 0.3 μm -channel HEMT by exposing the LED/HEMT epitaxial layers in selective area etching. The resulting monolithically integrated circuit shows a full gate voltage modulation of the light output power. This demonstrates compatibility of group-III nitride LED and HEMT processes. © 2013 AIP Publishing LLC. [<http://dx.doi.org/10.1063/1.4807125>]

GaN-based high-power light-emitting diodes (LEDs) used in lighting applications typically require dedicated electronic driver circuits for AC-DC power conversion, current sourcing, and dimming using pulse-width modulation (PWM) or analog current control methods.¹ GaN power switching field-effect transistors (FETs), such as metal-oxide-semiconductor (MOS) FETs, high-electron-mobility transistors (HEMTs), and MOS-Channel HEMTs (MOS-HEMTs) have shown outstanding performance in terms of high breakdown voltage (BV), low specific on-resistance, and high operating frequency,²⁻⁴ and can be very useful as output devices for emerging applications of high power–high voltage LED systems. Ultimately, monolithic integration of GaN-based LEDs and GaN power HEMTs can reduce the cost and the size of solid state lighting systems, improve system reliability, and serve as a technology platform for the development of light-emitting power integrated circuits (LEPICs). LEPICs can also play an important role in adding functionalities required for emerging solid state lighting applications such as visible light communication (VLC) and other LED control technologies required for future smart lighting applications.⁵

Monolithic integration of GaAs-based LEDs and GaAs MESFETs has been previously demonstrated;^{6,7} however, there has been no report on similar monolithic integration in GaN. Chilukuri *et al.* reported monolithic integration of AlGaInP LEDs with Si CMOS on lattice engineered SiGe wafers by regrowth of the LED epi.⁸ Liu *et al.* have reported monolithic integration of GaN LEDs arrays with Si CMOS using a flip chip method.⁹ Previously, we have proposed three different approaches for the integration of GaN

LEDs and HEMTs, including selective epi removal (SER), selective area growth (SAG), and 3-dimensional (3D) integration using GaN wafer bonding.¹⁰ In this paper, we report on the experimental demonstration of the monolithic integration of GaN LEDs and GaN HEMTs using the SER process approach.

Figure 1 shows the schematic cross-section of a monolithically integrated GaN LED and GaN MOSC-HEMT using the SER process. The starting HEMT epitaxial material was obtained from a commercial vendor with customized epi layers comprising 20 nm unintentionally doped (UID) GaN cap, on top of 20 nm of $\text{Al}_{0.23}\text{Ga}_{0.77}\text{N}$ barrier and on top of GaN buffer layers grown on a sapphire substrate. The LED epi was grown in-house on top of the HEMT epi using metal-organic vapor phase epitaxy (MOVPE). The LED epitaxial structure comprised 500 nm of N+ GaN, 90 nm UID GaN, 180 nm of a $\text{Ga}_{0.92}\text{In}_{0.08}\text{N}/\text{GaN}$ multiple quantum well (MQW) structure, 20 nm P+ AlGaIn, and 130 nm P+ GaN. The integrated LED and MOSC-HEMT structure was fabricated by first removing selected regions of the LED structure to expose the N+ GaN using Cl based inductively coupled plasma (ICP) reactive-ion etching (RIE). After the etching of

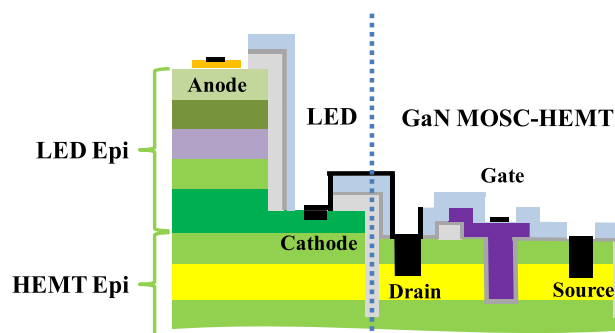


FIG. 1. Schematic cross-section view of the monolithically integrated GaN LED and GaN MOSC-HEMT using the SER approach.

^{a)}Electronic mail: liz6@rpi.edu. Tel.: +1 (518) 867 5427. Fax: +1 (518) 276 2990

^{b)}Present address: Silicon Power Corporation, Clifton Park, New York 12065, USA.

^{c)}Present address: School of Electrical and Computer Engineering, Georgia Institute of Technology, Atlanta, Georgia 30332, USA.

1.5 μm deep trenches around the exposed HEMT region for mesa isolation, the remaining N+ GaN layer on top of the HEMTs was selectively etched using ICP-RIE, and the etching was stopped within the 20 nm UID GaN cap. The 20 nm GaN cap provides extra tolerance for the N+ GaN etching stop point, and is intentionally left unetched as part of our high-voltage HEMT epi design for enhancing the BV of the MOSC-HEMTs.¹¹ 500 nm-thick plasma-enhanced chemical vapor deposition (PECVD) SiO₂ was subsequently deposited, densified, and patterned as field plate oxide. Next, the submicron recess channels of the MOSC-HEMTs were patterned using electron beam lithography, and etched using ICP-RIE followed by the wet etch in tetra-methyl-ammonium hydroxide (TMAH) at 85 °C for 15 min to remove dry etch damage. After cleaning, 50 nm SiO₂ was deposited as a gate dielectric using atomic layer deposition (ALD), followed by post-deposition annealing in an N₂ ambient at 1000 °C for 30 min. Polysilicon was then deposited using low pressure chemical vapor deposition (LPCVD), doped with POCl₃, and patterned as gate electrodes, followed by PECVD of 1000 nm-thick SiO₂ layer, which was densified as inter-layer dielectric (ILD). Ti/Al/Ni/Au was evaporated, lifted off, and annealed using rapid thermal annealing (RTA) at 800 °C for 1 min in N₂ to form the ohmic contacts of the GaN MOSC-HEMTs and the cathode contact of the GaN LEDs at the same time. Then thin Ni/Au was evaporated on top of the GaN LEDs followed by RTA at 500 °C for 1 min in O₂ to make the transparent P+ ohmic contact to the LED. Finally, Ti/Al was evaporated and patterned as the interconnect metal between GaN MOSC-HEMTs and GaN LEDs. Figure 2(a) shows an optical image of our fabricated monolithically integrated serially connected GaN LED/HEMT pair. The GaN LED cathode is connected to the MOSC-HEMT drain by interconnecting metal layer, forming a series configuration as shown in the inset of Figure 2(a). The LED/HEMT footprint ratio of the GaN HEMT area to the LED area shown in Figure 2 is 1.36, but mask design included integrated devices with a range of channel widths as well as designs using a single HEMT driving multiple serially connected LEDs, with the minimum footprint ratio as small as 0.09.

First, the basic I-V characteristics of the LED and HEMT elements were measured individually. Figure 3 shows the output I_D-V_D characteristics of the GaN MOSC-HEMT with channel length of 300 nm and channel width of 800 μm . Under a gate voltage of 16 V, the output current of

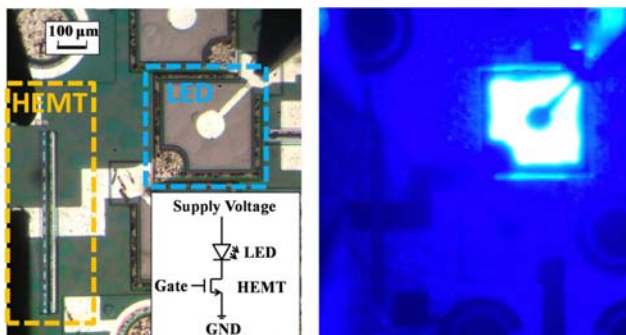


FIG. 2. Optical images of the monolithically integrated fabricated GaN LED/HEMT pair (a) in off-state, and (b) with the LED lighted up. Inset in (a): the schematic view of the circuit configuration.

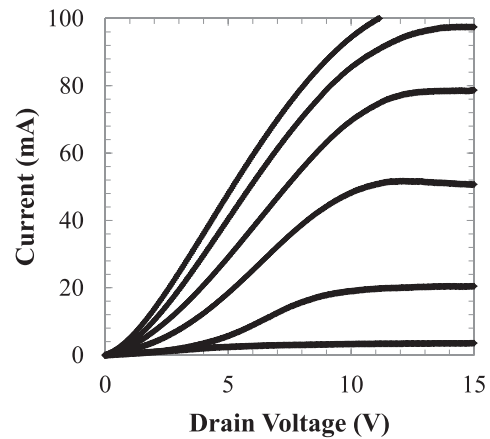


FIG. 3. Output I_D-V_D characteristics of the GaN MOSC-HEMT with channel length of 300 nm and width of 800 μm .

the HEMT reaches 100 mA, which is the maximum current limit of the testing equipment. The effects of the 20 nm UID GaN cap layer in the drift region of the HEMT were examined using numerical device simulation software MEDICI. The simulated band diagram and electron/hole carrier concentrations are shown in Figure 4. With the GaN cap layer, both the conduction band and the valence band in the AlGaIn bend upwards, resulting in the 2-dimensional hole gas (2DHG) at the GaN cap/AlGaIn interface along with the 2D electron gas (2DEG) at the AlGaIn/GaN interface. This simulation result was consistent with the previous experimental reports on the similar HEMT epi structure with 10 nm GaN cap layer.¹² The 2DEG is induced by the positive polarization charge (+Q_{pol}) at the bottom AlGaIn/GaN interface, and the 2DHG is induced by the negative polarization charge (-Q_{pol}) at the top GaN cap/AlGaIn interface, whose value is equal to that of the +Q_{pol} by nature.¹³ When the HEMT is off and both 2DEG and 2DHG are fully depleted, the +Q_{pol} and -Q_{pol} precisely counter balance each other. This perfect charge balancing yields a uniform surface field in the HEMT drift region, which enhances the breakdown voltage of the HEMT.¹⁴ Figure 5 shows the current and light output intensity vs voltage measured on a single 800 μm square GaN

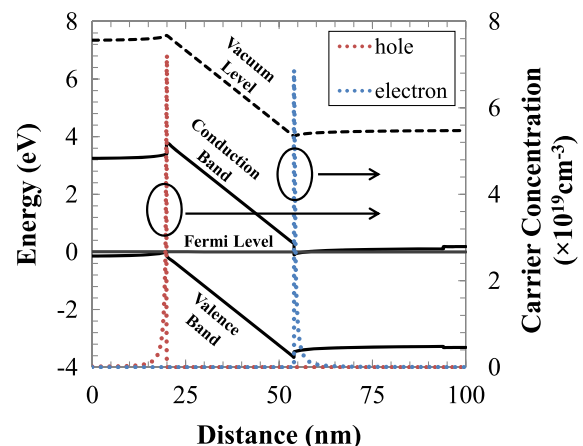


FIG. 4. Simulated band diagram and electron/hole concentration of the GaN HEMT epi with 20 nm UID GaN cap layer.

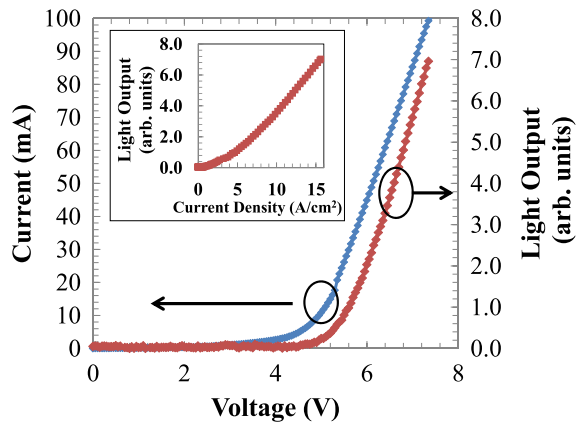


FIG. 5. Current and light output intensity vs voltage characteristics of the GaN LED with size of $800\ \mu\text{m} \times 800\ \mu\text{m}$. Inset shows the light output density vs current density characteristics.

LED. The light output intensity was measured using a simple photodiode detector. The light output intensity as a function of the current density is shown in the inset of Figure 5. Good linearity was observed for the low current density range explored in these measurements ($<20\ \text{A}/\text{cm}^2$).

Then the monolithically integrated GaN LED/HEMT pairs in serially connected configuration have been tested. No parasitic leakage between the LEDs and the HEMTs was observed, indicating effective isolation within our optimized mesa isolation process.¹⁵ As seen in Figure 2(b), the GaN LED emits bright blue light, when it is driven directly by the integrated GaN MOSC-HEMT. Figure 6 shows the LED current and the light output intensity as a function of the supply voltage and the HEMT gate voltage. The I-V characteristics of the integrated LED/HEMT pair are consistent with what is expected for a transistor connected in series with a diode, where the current is limited by the LED before it turns on, and by the saturation current of the transistor afterwards. The light output intensity shows that the LED light output has been fully modulated by the gate voltage of the MOSC-HEMT with good linearity.

In summary, we have demonstrated a GaN technology platform for fabricating monolithically integrated GaN LEDs and GaN power MOSC-HEMTs. The integration approach has been presented in detail, and the performance GaN MOSC-HEMTs, GaN LEDs, and the monolithically integrated GaN LED/HEMT pairs have been described. This work demonstrates that the electronic and opto-electronic properties of devices fabricated from (AlInGa)N and standard GaN device processing technologies are amenable to straightforward functional integration. The integration approach in this paper is but one of many possible approaches and can possibly be one of the basic building blocks of future LEPICs for many smart lighting applications.

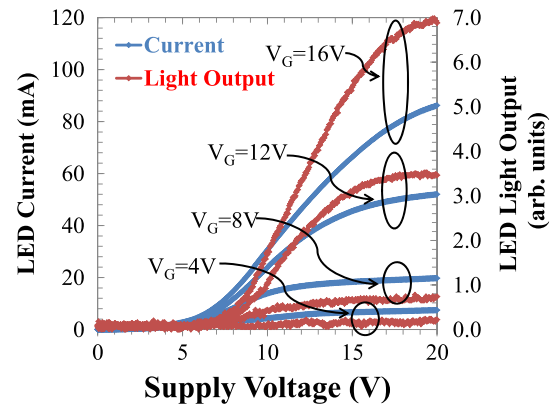


FIG. 6. LED current and light output intensity vs supply voltage, plotted as a function of the HEMT gate voltage.

This work was supported primarily by the Engineering Research Centers Program (ERC) of the National Science Foundation under NSF Cooperative Agreement No. EEC-0812056 and in part by New York State under NYSTAR Contract No. C090145. This work was performed in part at the Cornell NanoScale Facility, a member of the National Nanotechnology Infrastructure Network, which is supported by the National Science Foundation (Grant No. ECS-0335765).

¹H. Chiu, Y.-K. Lo, J.-T. Chen, S.-J. Cheng, C.-Y. Lin, and S.-C. Mou, *IEEE Trans. Ind. Electron.* **57**, 735 (2010).

²W. Huang, T. P. Chow, Y. Niiyama, T. Nomura, and S. Yoshida, in *Proceedings of International Symposium on Power Semiconductors Devices and ICs, Orlando, FL* (2008), p. 291.

³N.-Q. Zhang, B. Moran, S. P. DenBaars, U. K. Mishra, X. W. Wang, and T. P. Ma, *Phys. Status Solidi A* **188**, 213 (2001).

⁴B. Lu and T. Palacios, *IEEE Electron Device Lett.* **31**, 951 (2010).

⁵R. F. Karlicek, in *IEEE Photonics Society Summer Topical Meeting Series, Seattle, WA* (2012), p. 147.

⁶O. Wada, T. Sanada, and T. Sakurai, *IEEE Electron Device Lett.* **EDL-3**, 305 (1982).

⁷I. Polentier, L. Buydens, A. Ackaert, P. Demeester, P. van Daele, F. Depestel, D. Lootens, and R. Baets, *Electron. Lett.* **26**, 925 (1990).

⁸K. Chilukuri, M. J. Mori, C. L. Dohrman, and E. A. Fitzgerald, *Semicond. Sci. Technol.* **22**, 29 (2007).

⁹Z. J. Liu, K. M. Wong, C. W. Tang, and K. M. Lau, in *14th OptoElectronics and Communications Conference, Hong Kong, China* (2009).

¹⁰J. Waldron, R. F. Karlicek, and T. P. Chow, in *Proceedings of International Workshop on Nitride Semiconductors, Sapporo, Japan* (2012).

¹¹Z. Li, J. Waldron, R. Dayal, L. Parsa, M. Hella, and T. P. Chow, in *Proceedings of International Symposium on Power Semiconductors Devices and ICs, Bruges, Belgium* (2012), p. 45.

¹²A. Nakajima, Y. Sumida, M. H. Dhyani, H. Kawai, and E. M. S. Narayanan, *Appl. Phys. Express* **3**, 121004 (2010).

¹³O. Ambacher, B. Foutz, J. Smart, J. R. Shealy, N. G. Weimann, K. Chu, M. Murphy, A. J. Sierakowski, W. J. Schaff, L. F. Eastman, R. Dimitrov, A. Mitchell, and M. Stutzmann, *J. Appl. Phys.* **87**, 334 (2000).

¹⁴Z. Li and T. P. Chow, *Phys. Status Solidi C* **8**, 2436 (2011).

¹⁵Z. Li, J. Waldron, and T. P. Chow, in *Proceedings of the IEEE Lester Eastman Conference on High Performance Devices, Providence, RI* (2012).